

Salt-Induced Multilayer Growth: Correlation with Phase Separation in Solution

Vladimir Izumrudov,[†] Eugenia Kharlampieva, and Svetlana A. Sukhishvili*

Department of Chemistry and Chemical Biology, Stevens Institute of Technology,
Hoboken, New Jersey 07030

Received June 2, 2004; Revised Manuscript Received August 18, 2004

ABSTRACT: We report salt-induced phase separation of polyelectrolyte complexes in solution correlates with deposition of polymer multilayers at a surface. Multilayer growth was followed in situ using FTIR-ATR (Fourier transform infrared spectroscopy by attenuated total reflection). The polymer system was quaternized poly(4-vinylpyridine) (QPVP) and poly(methacrylic acid) (PMAA), with various ratios of PMAA to QPVP chain lengths. In solution, phase diagrams were produced for QPVP/PMAA mixtures containing excess of PMAA or QPVP, in both cases showing salt-induced phase separation. These phase diagrams controlled deposition of PMAA or QPVP chains at the surface and explained a bell-shaped dependence of the multilayer thickness on the salt concentration. The order of chain removal (occurring at the step of QPVP or PMAA deposition) could also be predicted from the phase state of QPVP/PMAA mixtures in solution. Finally, we show that, by using short equilibration times with solution, robust multilayers can be produced at surfaces even in conditions when multilayer deposition is aggravated by desorption of polymer chains.

Introduction

Alternating deposition of oppositely charged polyelectrolytes at a surface has been widely used to produce ultrathin polymer films—polyelectrolyte multilayers (PEMs).^{1–9} The mechanisms of film growth, structure of self-assembled film charge balance, and location of counterions have been the subjects of many studies.^{1–11} Polyelectrolyte multilayers are now considered to have a highly interpenetrated layered structure² that is mediated by a surface and reflects deposition history. Modern theories of PEM growth describe the buildup of these films as irreversible, in terms of amount deposited, successive deposition of layers.¹²

However, from the thermodynamic point of view, the fact that multilayer films can be successfully deposited at surfaces might seem to contradict the knowledge accumulated in the area of polyelectrolyte complexation in solution.¹³ During deposition, PEMs are exposed to a large excess, compared to film surface charge, of polyelectrolyte chains in solution whose charge is opposite to the charge of polymer included in the outermost layer of the film. These conditions are most favorable for the formation of water-soluble polyelectrolyte complexes (WPECs) in solution. The inclusion of a polyelectrolyte chain in WPEC should be more favorable, as compared to chain complexation at the surface for entropic reasons. Specifically, one expects gains in translational and configurational entropy due to an increase in number of WPEC species in solution and greater mobility of dissolved polyelectrolyte chains, respectively. WPECs based on carboxylate polyanions are particularly well studied,¹³ especially for the case of relatively low and moderate salt concentration, $[\text{NaCl}] < 0.3 \text{ M}$. Note that poly(carboxylic acid)s and their salts are often used to build PEMs.^{14–19} Studies of polyelectrolyte complexes showed that the ratio of positive-to-negative charge, calculated as a ratio of molar concentrations of repeat units, φ , is a critical parameter that determines the

phase behavior of the system.¹³ In the majority of systems studied, water-soluble complexes are formed when the excess of negative charge is large ($\varphi < 0.5$), and phase separation occurs as the charge excess decreases, with enhanced precipitation as φ approaches unity. It was shown that WPECs are thermodynamically stable structures, with a measurable chain transfer rate between molecularly dispersed complexes.²⁰ Specifically, in the case when the charge imbalance in the system is created by excess charge carried on a polyanion with a longer chain length, the WPECs contain, as a rule, only one chain of the longer polyelectrolyte.¹³ One could expect that, on the basis of thermodynamic arguments only, the growth of polyelectrolyte multilayers would be severely impeded if conditions favorable for the formation of WPEC are employed during the multilayer deposition. Desorption of polyelectrolytes from a multilayer resulting from competitive binding with polyelectrolyte chains in solution has also been reported by several authors.^{21–23} The connection between the phase behavior of polyelectrolyte complexes (PECs) in solution and polyelectrolyte complexes at a surface has been recently emphasized by Cohen Stuart and co-workers,²⁴ who suggested that deposition of multilayers at surfaces is largely controlled by the phase behavior of polyelectrolyte complexes in the absence of a substrate. Specifically, unstable film growth, or desorption of previously adsorbed polymer layers during deposition of the next polymer layer, was attributed to the formation of WPEC in solution. The effect of different salts, added at small concentrations, on the adsorption–desorption behavior of polyelectrolytes during multilayer buildup has been recently studied by Kovačević et al.²⁵

Nevertheless, the understanding of relationship between multilayer deposition and the phase diagrams of PEC complexes in solution has not yet matured to the level that allows one to rationally predict and control the transition between stable film growth and the deposition regime opposed by polymer desorption. It is also important that these predictions would be made for a wide range of conditions (ionic strength, ratio of chain length, etc.) usually used in multilayer deposition.

[†] Permanent address: Department of Polymer Chemistry, Moscow State University, 119992 Moscow, Russia.

* To whom correspondence should be addressed.

Table 1. Molecular Weights, Polymerization Degrees, and Chain Length Ratios of PMAA and QPVP

	M_w	M_w/M_n	DP _{QPVP} or DP _{PMAA}	$R = \text{DP}_{\text{PMAA}} / \text{DP}_{\text{QPVP}}$
QPVP	330K	1.10	1600	
PMAA, sodium salt	7K	1.07	65	0.04
PMAA, sodium salt	25K	1.05	230	0.14
PMAA	39K	1.05	450	0.28
PMAA	72K	1.05	850	0.53
PMAA, sodium salt	150K	1.11	1400	0.87
PMAA	350K	1.07	4050	2.53

Addition of salts to deposition solutions is often used to adjust the thickness of individual adsorbed layers constituting a multilayer film.^{3,26–28} An increase in ionic strength usually results in larger amounts of polymers adsorbed within PEMs at each deposition step. The formation of thicker layers is usually explained by analogy with behavior of a single layer of polyelectrolyte at a surface. In this line of argument, ionic strength screens electrostatic charges within polyelectrolyte chains, allowing larger amounts of polymer to be adsorbed at a surface. At high salt concentrations, multilayer destruction may also occur as a result of competition of small ions with ionic polymer–polymer pairing.^{3,29,30} For the case of a poly(carboxylic acid) self-assembled with a polycation, Schlenoff and co-workers have also recently reported an intriguing maximum in film thickness as a function of salt concentration.²⁹

In this paper, we contrast the deposition of poly(carboxylic acid)-containing multilayers at surfaces with the phase behavior of polyelectrolyte complexes in solution. Of special interest was to elucidate factors that control the interaction of oppositely charged chains in solution and at a surface, in particular the ratio of the polyelectrolyte chain lengths, charge imbalance, and ionic strength. We report results on the effect of the external salt on the phase behavior of polyelectrolyte complexes in solution under conditions that model multilayer deposition and show that this phase behavior to a large extent controls the observed dependence of the PEM thickness on the ionic strength.

Experimental Section

Materials. Polycation poly(*N*-ethyl-4-vinylpyridinium) bromide (QPVP) with $M_w = 330\,000$ was derived from poly(4-vinylpyridine) (PVP). PVP fractions were obtained by fractional precipitation in ethyl acetate/methanol solutions of a more polydisperse PVP sample obtained by radical polymerization. Narrow PVP fractions were dissolved in ethanol and precipitated in cold diethyl ether. A PVP sample with the weight-average degree of polymerization DP_{QPVP} of 1600 as measured by light scattering and low polydispersity index M_w/M_n of 1.10 as determined by GPC was quaternized with ethyl bromide in ethanol solution using well-established methods^{31,32} to obtain QPVP polymer with $96 \pm 2\%$ of pyridinium units as determined by infrared spectroscopy.

Poly(methacrylic acid) (PMAA) samples with varying degree of polymerization and narrow molecular weight distribution were purchased from the following sources: (a) American Polymer Standards (PMAA with M_w 72 000), (b) Polysciences, Inc. (PMAA, sodium salts with M_w 7000, 25 000, and 150 000), and (c) Polymer Standards Service GmbH (PMAA with M_w 350 000). PMAA with M_w 39 000 (as measured by light scattering) was obtained by radical polymerization of the methacrylic acid followed by fractional precipitation of this polymer in ethyl acetate/methanol mixtures. These samples are referenced below as PMAA7K, -25K, -39K, -72K, -150K, and -350K and have, as shown in Table 1, polymerization degrees DP_{PMAA} of 65, 230, 450, 850, 1400, and 4050, respectively.

To eliminate overlap of the IR spectra of polymers in the 1500–1700 cm^{-1} region with the strong water band, experi-

ments with multilayers were done in D₂O. D₂O with 99.9% isotope content was purchased from Cambridge Isotope Laboratories and was used as received. Though the acidity was determined by deuterium rather than hydrogen ions, we refer to it as pH rather than pD. To control ionic strength and pH, concentrated NaCl and Na₂HPO₄ buffer (General Storage, pure grade) were used as received. The H₂O used for glassware cleaning was deionized and further purified by passage through a Milli-Q system (Millipore).

Studies of Polyelectrolyte Complexes (PECs) in Solution. Water-soluble polyelectrolyte complexes (WPECs) were prepared by mixing 0.04 M aqueous solutions of QPVP and PMAA (concentrations of polymers are defined as molar concentrations of repeat units) at the ratios of positive-to-negative units of $\varphi = 0.2$ or $\varphi = 5.0$. Produced suspensions were dissolved by addition of 0.1 M aqueous NaOH to the point corresponding to the complete neutralization of carboxylic groups of PMAA and diluted with 0.01 M Na₂HPO₄ at pH 8.4. At this point, clear solutions of WPECs were formed.

Phase separation in WPEC solutions was then induced by adding 4 M aqueous NaCl and 0.01 M phosphate buffer (pH = 9) taken at certain proportions to achieve a final concentration of QPVP of 0.0025 M and a desired ionic strength. Precipitates were centrifuged at 2000 rpm, and the fraction of QPVP remaining in supernatants, QPVP_s, was determined by UV spectroscopy as the ratio $[\text{Abs}]_s/[\text{Abs}]_0$, where $[\text{Abs}]_s$ and $[\text{Abs}]_0$ are absorbancies at 257 nm measured with supernatant and with a reference 0.0025 M QPVP solution, respectively. For QPVP/PMAA mixtures with $\varphi = 0.2$, the data obtained were presented as a dependence of QPVP_s on salt concentration. For QPVP/PMAA mixtures with $\varphi = 5.0$, measured QPVP absorbances were recalculated to take into account the 5-fold excess of QPVP and the requirement for the separated phase to be neutral. In the latter case, a parameter QPVP_s* = $\{[\text{Abs}]_s - 0.8[\text{Abs}]_0\}/0.2[\text{Abs}]_0$ was used instead of QPVP_s to characterize the phase separation.

Sedimentation measurements of WPEC solutions were performed with a Beckman-E analytical ultracentrifuge at 48 000 rpm. The distribution of particles in a cell was estimated by a Schlieren optical system and, in parallel, by measuring the optical density of solutions in the cell at 260 nm corresponding to absorbance of QPVP. Note that PMAA does not absorb light at this wavelength.

Deposition of Multilayers. Multilayers were prepared on the surface of an oxidized ATR silicon crystal. The ATR surface was a rectangular Si crystal of dimensions 50 mm × 20 mm × 2 mm (Harrick Scientific) whose beam entrance and exit surfaces were cut at 45°. The methods to oxidize the crystal surface in a controlled way and to clean the cell elements were described elsewhere.³³ The silicon crystal was installed within a custom-made flow-through ATR–FTIR stainless steel cell. A polybase and a polyacid were then sequentially deposited in situ from 0.1 mg/mL solutions onto a surface of the silicon crystal. Measurements were done in D₂O solution containing 0.01 M phosphate buffer at pH 8.4. The deposition started from filling the cell with a pure buffer solution. The buffer solution was then replaced by a 0.1 mg/mL solution of QPVP in the same buffer. After waiting 20 min, the amount adsorbed reached a saturated value of $\sim 1.5 \text{ mg m}^{-2}$, and the polymer solution was replaced by a pure buffer at 0.01 M. PMAA was then deposited in a similar way, but from a buffer solution that additionally contained a desired concentration of NaCl. The NaCl concentration was kept constant throughout each deposition cycle and ranged from 0 to 0.5 M. All deposited films contained PMAA as the top layer.

FTIR-ATR Measurements. The amounts of polymers adsorbed and the degree of ionization of the carboxylic groups were quantified by in situ FTIR-ATR (Fourier transform infrared spectroscopy by attenuated total reflection) from the calibrated intensities of the vibrational bands of $-\text{COO}^-$, the pyridine and pyridinium rings using experimental protocols, and calibration methods described elsewhere.³⁴ Infrared spectra were collected using a Bruker Equinox-55 Fourier transform infrared (FTIR) spectrometer equipped with a narrow-band mercury cadmium telluride detector. Interferograms

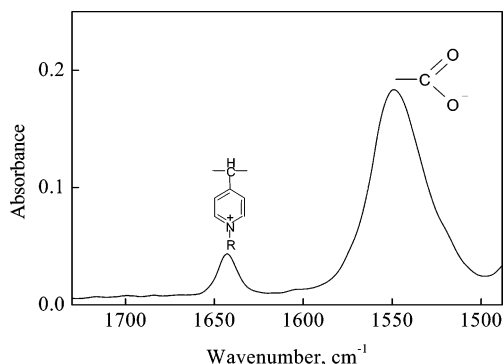


Figure 1. Representative FTIR-ATR spectrum of a nine-layer QPVP/PMAA film with PMAA ($M_w = 39K$) included in the top layer deposited in a buffer solution containing 0.25 M NaCl. Absorbance is plotted against wavenumber. The measurement was obtained in D_2O solution using 0.01 M phosphate buffer at pH 8.4. The spectrum was obtained by dividing the spectrum of the adsorbed multilayers by that of a Si crystal with a precursor layer in a pure buffer solution.

were collected at 4 cm^{-1} resolution, and the number of averaged scans was 120. To obtain the absorbance spectra analyzed below, each interferogram was divided by the corresponding background that was obtained with the ATR crystal covered by the precursor film (one-layer QPVP). Background spectra were measured at the same concentration of NaCl at which the multilayer deposition was performed.

In all experiments, the penetration depth of the evanescent wave was large relative to the thickness of the multilayers. For example, the penetration depth of the evanescent wave was 0.47 μm at 1643 cm^{-1} for the Si crystal that we used, and the largest thickness of a dry film we were working with was about 50 nm. This value is based on the adsorbed amount measured with the ATR-FTIR technique of about 50 $mg\ m^{-2}$ (assuming a density of a dry film of 1 $g\ cm^{-3}$) and does not take into account film swelling. However, even if the film thickness was increased due to swelling up to 100 nm (for the thickest film studied), the correction term for the decay of electric field with the distance from the surface of the crystal was estimated to be relatively small, about 10%, and was not introduced into calculations of the amount adsorbed.

Many measurements were performed in the presence of polymer solutions, but contributions from the polymer solution to the total signal did not exceed 1–2% for a solution concentration of 0.1 mg/mL .

The adsorbed amount of polymers and the degree of ionization of PMAA molecules within the multilayer were calculated from calibration constants which were independently determined by measuring the infrared absorbance of polymer solutions of known concentrations as they are brought into contact with a nonadsorbing surface. The detailed procedures include integration of intensity of the absorbing species in the evanescent wave as a function of distance from the crystal surface and have been described previously.^{35–37} Calibration of the amount adsorbed was also described in detail earlier for both QPVP and PMAA.³⁴ The calibration constants for QPVP and PMAA were 0.021 and 0.175 $abs\ units\ m^2\ mg^{-1}$, respectively.

Representative Spectra of the Multilayers. Figure 1 shows a representative infrared spectrum of a QPVP/PMAA film deposited on the Si surface at pH 8.4 and NaCl concentration of 0.25 M. The spectrum shows two major peaks: a band associated with in-ring skeletal vibrations of pyridinium rings at 1643 cm^{-1} and a band at 1552 cm^{-1} from the asymmetric stretching vibrations of the carboxylate groups (ν_a, COO^-). As seen in Figure 1, the FTIR-ATR spectrum of the multilayer does not contain the 1700 cm^{-1} $-COOH$ vibrational band, suggesting that PMAA is completely ionized under these conditions. This is consistent with pK_a of about 6–7 usually reported for PMAA. Although the use of D_2O instead of H_2O is known to slightly increase pK_a s of acidic groups as compared to their dissociation in water, this effect is small and usually

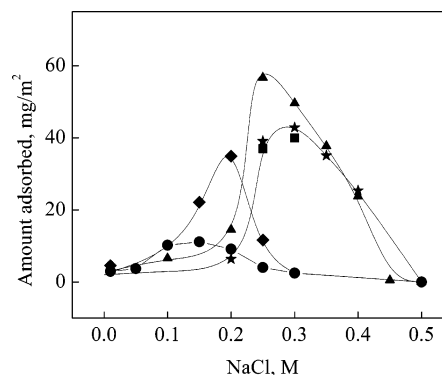


Figure 2. Total amount adsorbed of nine-layer QPVP/PMAA films deposited from solutions with various salt concentrations for different molecular weights of PMAA: 7K (circles), 25K (diamonds), 39K (triangles), 72K (squares), and 350K (stars). Multilayers were deposited from 0.1 mg/mL solutions at pH 8.4 created by phosphate buffer. The deposition time per layer was 1 h.

by about 0.2–0.6 pH units.³⁸ The intensities of the peaks shown in Figure 1 were then integrated using Galactic Grams/32 software. To determine the amount of adsorbed QPVP and PMAA molecules within the multilayer, we used the calibration constants listed in the previous section.

Results and Discussion

Self-Assembly of QPVP/PMAA Multilayers. The effect of ionic strength on sequential deposition of QPVP and PMAA with systematically varying ratio of chain lengths at the surface of a Si crystal is illustrated in Figure 2. In this paper the ratio of polyelectrolyte chain lengths, R , is defined as the ratio of the average number of repeat units in PMAA and QPVP chains. One QPVP sample with a M_w of 330K was used in all experiments, and the M_w of PMAA samples varied in a wide range from 7K to 350K. For each deposition cycle the multilayers shown in Figure 2 were exposed to 0.1 mg/mL PMAA or QPVP solutions for 60 min. During this time, the amount of polymer deposited almost reached its steady state, in some cases with some slower changes, ~5–8% of the amount deposited within a single layer, occurring for another hour. Three characteristic features are seen in Figure 2. First, the amount of polymer deposited goes through a maximum as a function of ionic strength. Second, especially for smaller molecular weights of PMAA, the position of this maximum shifts to higher ionic strengths when molecular weight of PMAA is increased. Finally, thicker multilayers are formed with longer PMAA chains. The maximum can be explained by the inclusion of counterions within the PEM followed by dissociation of the polyelectrolyte complex at high salt concentration. However, the data in Figure 2 show an intriguing feature that to our knowledge was not previously observed. In particular, for systems with high molecular weight of PMAA (39K and higher), multilayer growth was inhibited when the salt concentration was lower than 0.2 M NaCl, but robust multilayers were produced when the salt concentration was increased in a narrow range from 0.2 to 0.25 M NaCl. In this interval of ionic strength, the changes in the electrostatic screening length are small, from 7 to 6 Å, and cannot explain the observed sharp increase in the adsorbed amount.

Nevertheless, electrostatic screening does play a role in film deposition. Clues about the possible role of electrostatic screening on film deposition were obtained

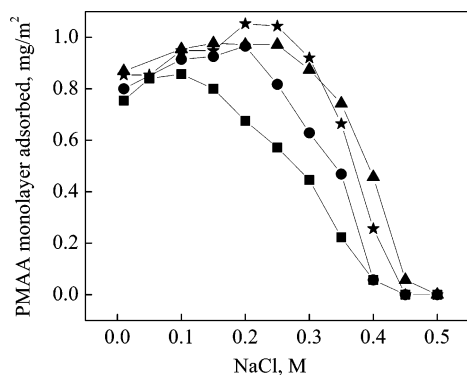


Figure 3. Amount adsorbed within a single PMAA layer deposited onto QPVP-pretreated surface of a Si crystal as a function of ionic strength for different molecular weights of PMAA: 7K (squares), 25K (circles), 39K (triangles), and 350K (stars). Each amount adsorbed was obtained in a separate experiment. The amount of QPVP deposited within a precursor layer was ~ 1.5 mg/m². Conditions used in the depositions are the same as in Figure 2.

in a series of control experiments that involved measurements of the amounts of PMAA deposited on the surface of the QPVP-covered substrate at various salt concentrations. Note that the amount of QPVP included within a precursor layer onto a substrate was the same in experiments involving various ionic strengths, signifying that no desorption of QPVP chains (adsorbed at low ionic strength conditions at pH 8.4) occurred in solutions with salt concentration up to 0.5 M NaCl. The results of deposition of PMAA onto a QPVP-covered surface of silicon crystal are shown in Figure 3. In contrast to multilayer buildup shown in Figure 2, polymer deposition occurs from a buffer solution in the absence of added salt, and an increase in the salt concentration results in a 5–20% increase in the amount adsorbed. A similar increase in mass adsorbed of 5–20%, in a range of salt concentration from 0 to 0.15–0.3 M NaCl, was also obtained for the QPVP layer adsorbed on top of the first PMAA layer (data not shown). The latter increase can be attributed to the enhanced screening of electrostatic charges within the adsorbed layer. At salt concentrations higher than a certain value (this value was within a range from 0.15 to 0.3 M NaCl for QPVP/PMAA systems with various molecular weights of PMAA), PMAA and QPVP mass adsorbed decreased because of enhanced screening of electrostatic interactions between surface charges, QPVP and PMAA chains. The latter is in good agreement with data reported earlier on the association of PMAA and QPVP in salt solutions¹³ and PEMs constructed from carboxylate polyanions and quaternized polyamines.²⁹ The difference between polymer deposition within the first adsorption layers and within the multilayer is explained by pinning of the first polymer layers to a solid surface, resulting, for example, in extremely sluggish kinetics of exchange of polymer chains.^{39,40} In the case of polyelectrolyte multilayers, the effect of a solid surface decays with the number of layers, since the later deposited chains adhere only due to polymer–polymer interactions.

Seeking to understand salt-induced multilayer growth, we turned our attention to studies of polyelectrolyte complexes (PEC) in solution. Note that salt-containing solutions are the most relevant for studies of multilayers since small ions are often added in large amounts to promote multilayer growth.^{2,26,27} Experiments involving

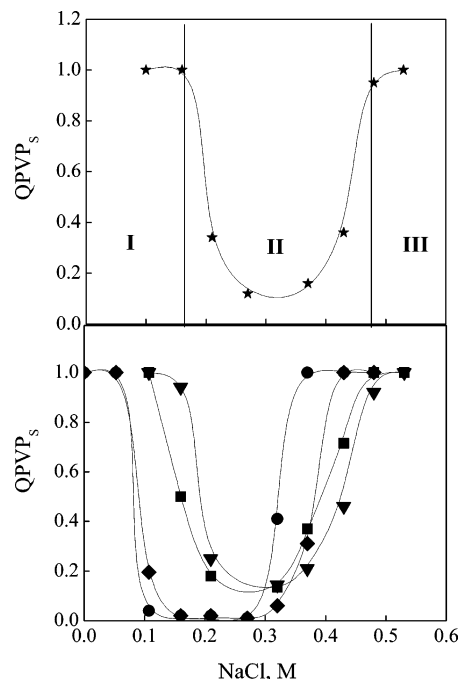


Figure 4. Fraction of QPVP, QPVP_s, remaining in supernatants of QPVP/PMAA mixtures for PMAA with different molecular weights [350K (top panel); 7K (circles), 25K (rhombuses), 72K (squares), and 150K (triangles) (bottom panel)] plotted against salt concentration. The ratio of charged units in the QPVP/PMAA mixtures, φ , was 0.2 (5-fold PMAA excess).

PEC in solution were designed to mimic conditions employed during multilayer deposition. We were specifically interested to explore PEC of the following compositions: (1) large excess of polyanion ($\varphi \ll 1$) and (2) large excess of polycation ($\varphi \gg 1$). The top panel in Figure 4 shows, for the longest PMAA chains ($R \sim 2.53$) present in excess ($\varphi = 0.2$), a fraction of QPVP, QPVP_s, remaining in the supernatant after separation of the precipitate from QPVP/PMAA mixtures containing varying amounts of salt. One sees that while at low salt concentrations all QPVP chains are solubilized in aqueous solution (region I), an increase in ionic strength promotes phase separation in the system (region II). It is important to note that the transition from region I to region II was completely reversible and fast, in good agreement with previously reported fast kinetics of chain exchange in PEC complexes in salt solution.²⁰ Salt-induced phase separation in the QPVP/PMAA system has been reported earlier for a system containing relatively short QPVP chains.¹³ In this transition region, the increase in ionic strength induces redistribution of QPVP between PMAA chains, producing PMAA-enriched (soluble) and PMAA-depleted (insoluble) polyelectrolyte complexes. This intriguing experimental observation is still poorly understood, probably (at least in part) due to the structural complexity of water–salt solutions.⁴¹ A mechanism for the salt-induced phase separation that considers the WPEC contraction due to screening of unbound PMAA charges by the added salt and cooperative chain rearrangements at the point of phase separation caused by high local ionic strength was recently proposed.⁴² Finally, at even higher salt concentration the precipitate dissolves (region III) due to dissociation of the system of intermolecular contacts between PMAA and QPVP chains.

In contrast to systems with long PMAA chains (large R), PECs that contain shorter PMAA ($R \ll 1$) show

significantly different phase behavior. These data for QPVP/PMAA systems with various ratios of chain lengths are shown in the bottom panel of Figure 4. Two points are evident in Figure 4. First, with short PMAA chains (PMAA7K) the onset of phase separation occurs at a significantly lower critical salt concentration. These critical values were 0.08 and 0.18 M NaCl for the QPVP/PMAA system with PMAA7K and PMAA350K, respectively. Second, in the phase-separated region (region II), with shorter PMAA chains (PMAA7K and PMAA25K), all QPVP chains are included in the precipitate. From the ratio of total number of positive-to-negative charges in the polymer chains $\varphi = 0.2$ and the requirement for separated phases to be neutral, one can calculate that 80% of PMAA chains remain in the supernatant and are not associated with QPVP. At the same time, in the case of longer PMAA chains, the precipitate coexists with water soluble QPVP/PMAA complex. To explain the failure of short chains to solubilize the long polycation chains, an argument can be made that the formation of a water-soluble complex with shorter PMAA chains is energetically unfavorable because of the large entropic loss in translational and configurational entropy that accompanies immobilization of large numbers of PMAA chains on the polycation. A significant piece of evidence in support of this argument was obtained in our studies of sedimentation coefficients of the particles using ultracentrifugation, as described in the Experimental Section. Specifically, QPVP/PMAA mixtures with composition $\varphi = 0.2$ were studied at salt concentrations lower than those inducing phase separation. In systems with long PMAA chains (PMAA350K), QPVP/PMAA mixtures showed only one sedimentation boundary in both Schlieren and UV scans, corresponding to a WPEC whose composition φ coincides with the composition of the mixture. In contrast, in mixtures containing PMAA7K, there were two boundaries in the Schlieren traces, whereas the UV-scanning pattern showed only one boundary. This finding suggests that even at low salt concentration (in region I) the mixtures were not homogeneous; i.e., WPEC coexisted with a significant proportion of PMAA chains that were not associated with QPVP chains.

Comparison of the data on phase separation of PECs in solution (Figure 4) with those on multilayer growth at a surface (Figure 2) shows that the data on the amount of insoluble PEC produced at each R and the amount of polymers deposited within the multilayers seem to be in disagreement. Specifically, with short PMAA chains, the amount of insoluble complex is the largest (see Figure 4), but the amount deposited at the surface is very small, ~ 1 Å at the deposition maximum for the system with PMAA7K (Figure 2). This seeming contradiction can be resolved when one takes into account that the phase diagram obtained at $\varphi \ll 1$ models only one of the two growth steps of a QPVP/PMAA film, namely the deposition of a polyanion. A second step in multilayer deposition, adsorption of QPVP, corresponds to large φ values ($\varphi \gg 1$). This latter situation was modeled in a different experiment on phase separation of PEC in solution, in which a constant and large excess of a polycation was sustained. Figure 5 shows the phase diagram of QPVP/PMAA solutions with $\varphi = 5$, shown as a dependence of QPVP_S* on salt concentration for various R . One can see that in all QPVP/PMAA systems the excess of QPVP charges solubilizes QPVP/PMAA complex in 0.01 M buffer

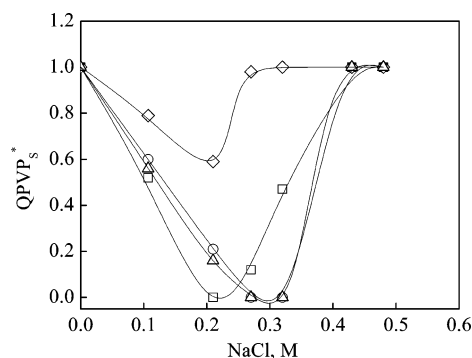


Figure 5. Fraction of QPVP, QPVP_S*, remaining in supernatants of QPVP/PMAA mixtures for PMAA with different molecular weights [7K (rhombuses), 25K (squares), 72K (circles), and 350K (triangles)] plotted against salt concentration. The ratio of charged units in the QPVP/PMAA mixtures, φ , was 5 (5-fold QPVP excess).

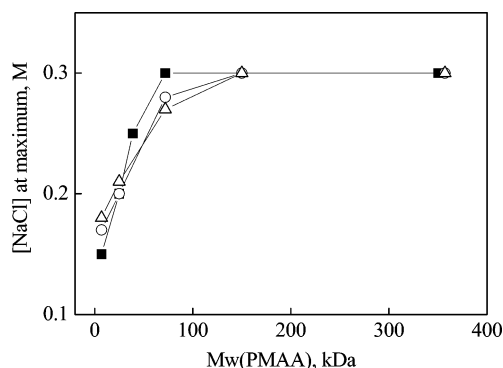


Figure 6. Salt concentrations corresponding to (a) maximum precipitation of QPVP from solution as determined from the data in Figure 4 in PMAA excess (open circles) and in Figure 5 in QPVP excess (open triangles) and (b) maximum in amount adsorbed as determined from data in Figure 2 (filled squares).

solution that did not contain sodium chloride. However, in salt solutions, significant precipitation occurred at all ratios of PMAA to QPVP chain lengths. Note that for the shortest polyacid (PMAA7K) the amount of precipitate at any given ionic strength was much smaller than that for longer PMAA chains, and at the point of maximum precipitation, at least 60% of QPVP was included in WPEC. Also seen in Figure 5 is that for larger molecular weights of PMAA maximum precipitation occurred at higher NaCl concentrations.

Figure 6 summarizes the results on phase separation in solution and multilayer deposition at a surface. As seen in Figure 6, maximum precipitation in the QPVP/PMAA mixtures with an excess of polycation or polyanion, and the largest amount of polymers deposited within the multilayer occurs at the same concentration of salt. This result shows direct correlation between phase separation in PEC solutions and multilayer growth at surfaces. It should be mentioned that our selection of ratio of QPVP to PMAA concentration in solution was largely dictated by the choice of technique used to analyze the composition of phases and might not necessarily reflect the real excess of positive or negative charges during multilayer deposition. Specifically, we have found that the value of the ionic strength inducing phase separation of QPVP/PMAA complexes in solution is also dependent on the total ratio of QPVP to PMAA units, φ . This effect, however, is relatively weak, especially for small R values, and in our experiment a very good agreement was obtained on the ionic strength scale between solution and surface data.

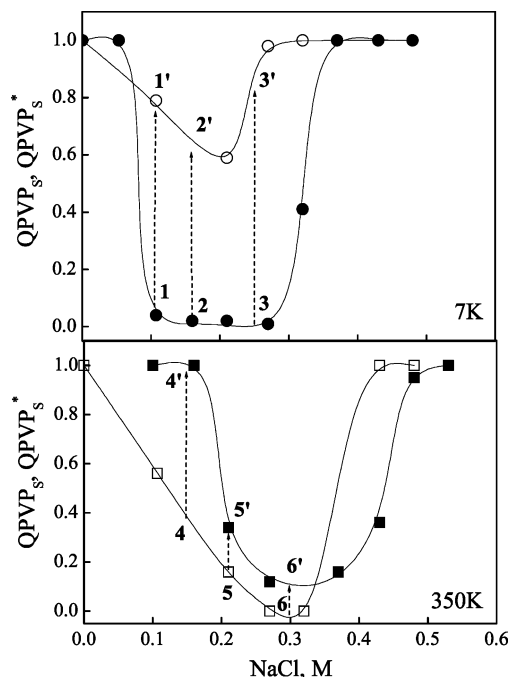


Figure 7. Top panel: fraction of QPVP remaining in supernatants of QPVP/PMAA mixtures containing PMAA7K in excess of PMAA (filled circles), QPVP_s, and in excess of QPVP (open circles), QPVP_s*, plotted against concentration of the added salt. Bottom panel: fraction of QPVP remaining in supernatants of QPVP/PMAA mixtures for PMAA with M_n of 350K in excess of PMAA (filled squares) and in excess of QPVP (open squares) plotted against concentration of the added salt. Arrows indicate, for a certain ionic strength, a mismatch in QPVP/PMAA phase diagrams obtained in excess of QPVP or PMAA.

We suggest that during deposition of PMAA or QPVP within a multilayer polymer deposition and multilayer growth are controlled, in an alternating way, by phase diagrams with $\varphi < 1$ or $\varphi > 1$. This is illustrated in Figure 7 where phase diagrams obtained for an excess of polyanion and an excess of polycation are plotted for two different PMAA chain lengths. Figure 7, top panel, shows that with the shortest, PMAA7K, chains, complete precipitation of QPVP chains occurs in an excess of PMAA (lower curve), but a significant fraction of QPVP is solubilized when QPVP is added in excess (upper curve). On the basis of these phase diagrams, one can predict that at this ratio of chain lengths the deposition of short PMAA chains will occur at ionic strengths 0.1–0.25 M (points 1–3 in Figure 7, top panel) but that the adsorbed polyacid will be removed at the step of the QPVP deposition (points 1'–3'). This prediction is confirmed by in situ ATR–FTIR experiments on deposition of QPVP/PMAA multilayers illustrated in Figure 8 (curves 1–3). One can see that ~70–90% of low molecular weight PMAA initially deposited at ionic strengths from 0.1 to 0.25 was removed from the surface after 20 min when the multilayer was brought into contact with QPVP solution. The inset in Figure 8 contrasts the rates of QPVP binding at the multilayer surface and PMAA chain removal. There is a distinct overshoot in the amount of QPVP deposited, originating from two successive kinetic processes: QPVP binding with surface PMAA chains followed by solubilization of previously adsorbed PMAA chains and desorption of WPEC in solution.

For QPVP/PMAA with longer polyacid chains (PMAA350K), the phase diagrams shown in Figure 7,

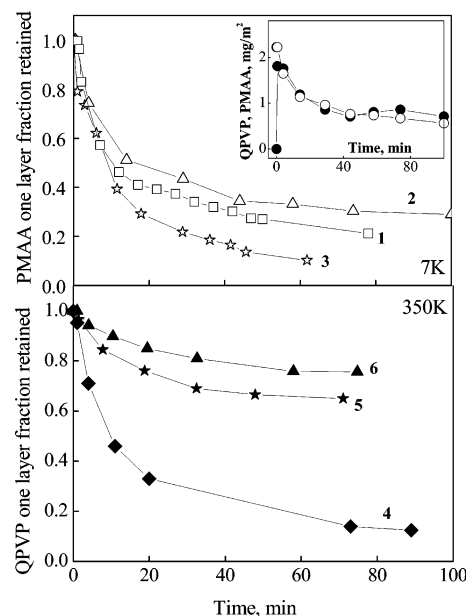


Figure 8. Top panel: desorption of a top PMAA layer during deposition of a QPVP layer on top of a seven-layer QPVP/PMAA7K film at different concentrations of NaCl: 0.1 (curve 1), 0.15 (curve 2), and 0.25 M (curve 3). Inset compares the elution of PMAA and QPVP adsorbed amounts (open and filled circles, respectively) within the top two layers during deposition of QPVP at 0.15 M NaCl concentration. Bottom panel: desorption of a top QPVP layer at the step of deposition of PMAA onto an eight-layer QPVP/PMAA350K film at different concentrations of NaCl: 0.15 (curve 4), 0.2 (curve 5), and 0.3 M (curve 6).

bottom panel, suggest the opposite desorption behavior during multilayer growth. As seen in Figure 7, bottom panel, at ionic strengths 0.15–0.35 M NaCl stronger precipitation occurs in excess of QPVP (lower curve) and solubilization is more pronounced in excess PMAA (upper curve), especially at sodium chloride concentrations smaller than 0.2 M NaCl. In the latter case, one can predict the stable deposition of QPVP chains within the multilayer, followed by removal of adsorbed QPVP chains in the PMAA solution (points 4 and 4' in Figure 7). This expectation is confirmed by kinetics data shown for salt concentration of 0.15 M NaCl (curve 4 in Figure 8). The phase diagrams in Figure 7, bottom panel, also predict that an increase in salt concentration should result in the inhibition of desorption and stabilization of multilayer growth (points 5/5' and 6/6'). The bottom panel in Figure 8 confirms that during deposition of PMAA350K on top of a QPVP-capped eight-layer film desorption of QPVP chains was suppressed when the ionic strength was increased from 0.15 to 0.2 in 0.3 M NaCl.

The removal of previously adsorbed polymer chains, however, occurs over a time scale of minutes (inset in Figure 8) and can be stopped when polymer solution is replaced with pure buffer at early stages of desorption. This nonequilibrated polymer deposition can be used for multilayer buildup. Figure 9 shows that when only 5 min is allowed for equilibration, an incremental increase in total mass occurs at each deposition step, and the multilayers can be successfully built. When a large time is allowed for equilibration of the multilayer with solution, the removal of the top PMAA adsorbed layer in an excess of QPVP chains progressed, resulting in the oscillations of total mass deposited within the film.

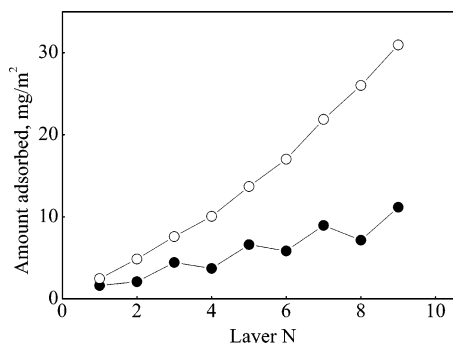


Figure 9. Evolution of total amount of QPVP and PMAA adsorbed during the buildup of a nine-layer QPVP/PMAA7K film deposited from solutions containing 0.15 M NaCl, with deposition time per layer of 5 min (open circles) and 1 h (filled circles). Odd layer numbers correspond to deposition of PMAA and even numbers to deposition of QPVP.

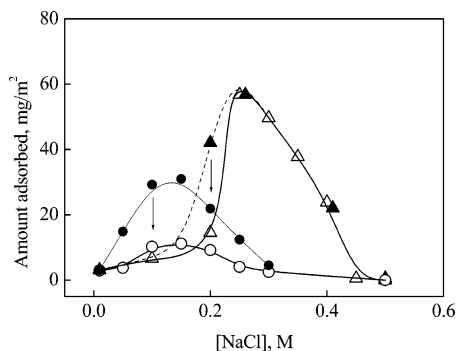


Figure 10. Total amount adsorbed of nine-layer QPVP/PMAA films deposited at pH 8.4 from solutions with various salt concentrations for PMAA39K (triangles) and PMAA7K (circles). The deposition time per layer was 5 min (filled symbols) and 1 h (open symbols). Arrows show evolution of the amount adsorbed when longer time was allowed for equilibration with solution at each deposition step.

The effect of the deposition time, for short and long equilibration times, on multilayer thickness is contrasted in Figure 10. One can see that, especially in the case of low molecular weight PMAA7K, much thicker films are produced if only 5 min is allowed for equilibration with solution at each deposition step. With 60 min allowed for adsorption, much thinner films could be deposited at the surface at any given ionic strength. For high molecular weight polyacid (PMAA39K), the strongest effect of deposition time on mass adsorbed was observed at salt concentrations of about 0.15–0.2 M, and multilayer thicknesses did not vary with deposition time at higher concentrations of salt. In experiments with both molecular weights of PMAA, an increase in deposition time resulted in evolution of the multilayer thicknesses toward those predicted thermodynamically based on the shapes of QPVP/PMAA phase diagrams in solution.

In summary, we demonstrate that the phase behavior of polyelectrolyte complexes in solution largely determines multilayer growth at surfaces. Specifically, the ionic strength dependence of the deposition of a polycation and a weak polyanion at surfaces can be understood from studies of salt-induced phase separation in polyelectrolyte mixtures in solution. We suggest that by using this approach the mode of multilayer growth in the systems studied here, as well as many others that involve weak or permanently charged polyelectrolytes,

proteins, nanoparticles, and many other systems, can be rationally predicted and controlled.

Acknowledgment. This work was supported by the National Science Foundation under award DMR-0209439 as well as through an CEEP international supplement to this award.

References and Notes

- (1) Decher, G.; Hong, J.-D. *Makromol. Chem., Macromol. Symp.* **1991**, *46*, 321.
- (2) Decher, G. *Science* **1997**, *277*, 1232.
- (3) Bertrand, P.; Jonas, A.; Laschewsky, A.; Legras, R. *Macromol. Rapid Commun.* **2000**, *21*, 319.
- (4) Schlenoff, J. B.; Dubas, S. T. *Macromolecules* **2001**, *34*, 592.
- (5) Gaul, W. G.; Li, M.; Schlenoff, J. B. *J. Phys. Chem. B* **1999**, *103*, 2718.
- (6) Dubas, S. T.; Schlenoff, J. B. *Macromolecules* **1999**, *32*, 8153.
- (7) Sukhorukov, G. B.; Möhwald, H.; Decher, G.; Lvov, Y. M. *Thin Solid Films* **1996**, *284–285*, 220.
- (8) Kotov, N. A.; Magonov, S.; Tropsha, E. *Chem. Mater.* **1998**, *10*, 886.
- (9) Fisher, P.; Laschewsky, A.; Wischerhoff, E.; Arys, X.; Jonas, A.; Legras, R. *Macromol. Symp.* **1999**, *137*, 1.
- (10) Schlenoff, J. B.; Dubas, S. T. *Macromolecules* **2001**, *34*, 592.
- (11) Gaul, W. G.; Li, M.; Schlenoff, J. B. *J. Phys. Chem. B* **1999**, *103*, 2718.
- (12) Casrelino, M.; Joanny, J.-F. *Langmuir* **2000**, *16*, 7524.
- (13) Kabanov, V. A. *J. Polym. Sci.* **1994**, *36*, 143.
- (14) Shiratori, S. S.; Rubner, M. F. *Macromolecules* **2000**, *33*, 4213.
- (15) Müller, M.; Rieser, T.; Lunkwitz, K.; Berwald, S.; Meier-Haack, J.; Jehnichen, D. *Macromol. Rapid Commun.* **1998**, *19*, 333.
- (16) Yoo, D.; Shiratori, S. S.; Rubner, M. F. *Macromolecules* **1998**, *31*, 4309.
- (17) Chen, K. M.; Jiang, X. P.; Kimerling, L. C.; Hammond, P. T. *Langmuir* **2000**, *16*, 7825.
- (18) Dubas, S. T.; Farhat, T. R.; Schlenoff, J. B. *J. Am. Chem. Soc.* **2001**, *123*, 5368.
- (19) Cao, T.; Chen, J.; Yang, Ch.; Cao, W. *Macromol. Rapid Commun.* **2001**, *22*, 181.
- (20) Bakeev, K. N.; Izumrudov, V. A.; Kuchanov, S. I.; Zezin, A. B.; Kabanov, V. A. *Macromolecules* **1992**, *25*, 4249.
- (21) Hoogeveen, N. G.; Cohen Stuart, M. A.; Fleer, G. J.; Böhmer, M. R. *Langmuir* **1996**, *12*, 3675.
- (22) Sui, Z.; Salloum, D.; Schlenoff, J. B. *Langmuir* **2003**, *19*, 2491.
- (23) Schoeler, B.; Kumaraswamy, G.; Caruso, F. *Macromolecules* **2002**, *35*, 889.
- (24) Kovačević, D.; Van der Burgh, S.; de Keizer, A.; Cohen Stuart, M. A. *Langmuir* **2002**, *18*, 5607.
- (25) Kovačević, D.; van der Burgh, S.; de Keizer, A.; Cohen Stuart, M. A. *J. Phys. Chem. B* **2003**, *107*, 7998.
- (26) Lvov, Yu.; Decher, G.; Haas, H.; Möhwald, H.; Kalachev, A. *Physica B* **1994**, *198*, 89.
- (27) Schlenoff, J. B.; Ly, H.; Li, M. *J. Am. Chem. Soc.* **1998**, *120*, 7626.
- (28) Tronin, A.; Lvov, Y.; Nicolini, C. *Colloid Polym. Sci.* **1994**, *272*, 1317.
- (29) Dubas, S. T.; Schlenoff, J. B. *Macromolecules* **2001**, *34*, 3736.
- (30) Dubas, S. T.; Farhat, T. R.; Schlenoff, J. B. *J. Am. Chem. Soc.* **2001**, *123*, 5368.
- (31) Fuoss, R. M.; Strauss, U. P. *J. Polym. Sci.* **1948**, *3*, 246.
- (32) Margolin, A. L.; Izumrudov, V. A.; Švedas, V. K.; Zezin, A. B.; Kabanov, V. A.; Berezin, I. V. *Biochim. Biophys. Acta* **1981**, *660*, 359.
- (33) Frantz, P.; Granick, S. *Macromolecules* **1995**, *28*, 6915.
- (34) Kharlampieva, E.; Sukhishvili, S. A. *Langmuir* **2003**, *19*, 1235.
- (35) Sperline, R. R.; Maralidharan, S.; Feiser, H. *Langmuir* **1987**, *3*, 198.
- (36) Harrick, N. J. *J. Opt. Soc. Am.* **1965**, *55*, 851.
- (37) Azzopardi, M. J.; Arribart, H. *J. Adhes.* **1994**, *46*, 103.
- (38) Salomaa, P.; Schaleger, L. L.; Long, F. A. *J. Am. Chem. Soc.* **1964**, *86*, 1.
- (39) Johnson, H. E.; Granick, S. *Science* **1992**, *255*, 966.
- (40) Sukhishvili, S. A.; Granick, S. *J. Chem. Phys.* **1998**, *109*, 6869.
- (41) Leberman, R.; Soper, A. K. *Nature (London)* **1995**, *378*, 364.
- (42) Izumrudov, V. A.; Lim, S. H. *J. Polym. Sci.* **1998**, *A40*, 276.